Rapid sealing of porcine renal blood vessels, *ex vivo*, using a high power, 1470-nm laser, and laparoscopic prototype

Luke A. Hardy
Thomas C. Hutchens
Eric R. Larson
David A. Gonzalez
Chun-Hung Chang
William H. Nau
Nathaniel M. Fried

Rapid sealing of porcine renal blood vessels, *ex vivo*, using a high power, 1470-nm laser, and laparoscopic prototype

Luke A. Hardy,[a] Thomas C. Hutchens,[a] Eric R. Larson,[b] David A. Gonzalez,[a] Chun-Hung Chang,[a] William H. Nau,[b] and Nathaniel M. Fried[a,*]
[a]University of North Carolina at Charlotte, Department of Physics and Optical Science, Charlotte, North Carolina, United States
[b]Medtronic, Boulder, Colorado, United States

Abstract. Energy-based, radiofrequency (RF) and ultrasonic (US) devices currently provide rapid sealing of blood vessels during laparoscopic procedures. We are exploring infrared lasers as an alternate energy modality for vessel sealing, capable of generating less collateral thermal damage. Previous studies demonstrated feasibility of sealing vessels in an *in vivo* porcine model using a 1470-nm laser. However, the initial prototype was designed for testing in open surgery and featured tissue clasping and light delivery mechanisms incompatible with laparoscopic surgery. In this study, a laparoscopic prototype similar to devices currently in surgical use was developed, and performance tests were conducted on porcine renal blood vessels, *ex vivo*. The 5-mm outer-diameter laparoscopic prototype featured a traditional Maryland jaw configuration that enables tissue manipulation and blunt dissection. Laser energy was delivered through a 550-μm-core-diameter optical fiber with side-delivery from the lower jaw and beam dimensions of 18-mm length × 1.2-mm width. The 1470-nm diode laser delivered 68 W with 3-s activation time, consistent with vessel seal times associated with RF and US-based devices. A total of 69 fresh porcine renal vessels with mean diameter of 3.3 ± 1.7 mm were tested, *ex vivo*. Vessels smaller than 5-mm diameter were consistently sealed (48/51) with burst pressures greater than malignant hypertension blood pressure (180 mmHg), averaging 1038 ± 474 mmHg. Vessels larger than 5 mm were not consistently sealed (6/18), yielding burst pressures of only 174 ± 221 mmHg. Seal width, thermal damage zone, and thermal spread averaged 1.7 ± 0.8, 3.4 ± 0.7, and 1.0 ± 0.4 mm, respectively. Results demonstrated that the 5-mm optical laparoscopic prototype consistently sealed vessels less than 5-mm diameter with low thermal spread. Further *in vivo* studies are planned to test the performance across a variety of vessels and tissues. © *2017 Society of Photo-Optical Instrumentation Engineers (SPIE)* [DOI: 10.1117/1.JBO.22.5.058002]

Keywords: arteries; blood vessels; burst pressure; coagulation; infrared; laparoscopic; laser.

Paper 170094PR received Feb. 10, 2017; accepted for publication Apr. 28, 2017; published online May 27, 2017.

1 Introduction

1.1 Energy-Based Surgical Devices

Suture ligation of blood vessels and tissue structures during open and laparoscopic surgery is both time consuming and skill intensive. The use of energy-based devices enables more rapid and efficient vessel and tissue ligation to maintain hemostasis during surgery than standard sutures and mechanical clips, which leave foreign objects in the body. These energy-based devices can reduce surgical operative times and costs significantly.[1–6] The majority of energy-based devices are powered by ultrasonic (US) or radiofrequency (RF) energy. US devices are indicated for thermal coagulation and cutting of vessels up to 5 mm in diameter.[7,8] RF devices can be used with larger vessels, but in practice, most clinicians are hesitant to use energy-based devices on vessels greater than 5 mm in diameter. A main concern when using energy-based devices is the possibility of unintended thermal damage to adjacent critical tissue structures when performing delicate procedures in confined spaces (e.g., prostatectomies and thyroidectomies). The active jaw of US devices can reach temperatures in excess of 200°C

during an application and can take greater than 20 s to cool to usable temperatures before proceeding with further applications. The maximum temperatures on the active jaw of RF devices are lower, less than 100°C, but larger thermal spread is observed.[9,10] These US and RF energy-based devices expedite a number of traditionally labor-intensive surgical procedures, such as lobectomy,[11] nephrectomy,[3] gastric bypass,[12] splenectomy,[13] thyroidectomy,[14] hysterectomy,[15] and colectomy.[16] However, both electrosurgical and US devices have limitations, including potential for undesirable charring and unnecessarily large collateral thermal damage zones, with thermal spread beyond the seal zone averaging greater than 1 mm.[17–20]

1.2 Infrared Laser Vessel Sealing

Our laboratory is currently exploring infrared (IR) lasers as an alternative energy modality for vessel sealing, capable of generating less collateral thermal damage.[21,22] Previous studies demonstrated the feasibility of sealing vessels in an open *in vivo* porcine model using a 1470-nm diode laser.[23] However, the initial prototype was designed for testing in open surgery and featured a plunger style tissue clasping mechanism and 12.7-mm

outer-diameter optical components in the light delivery mechanism that were incompatible with standard laparoscopic surgical instruments and size constraints. In this study, an optical laparoscopic prototype with 5-mm-outer-diameter shaft was integrated within a standard Maryland jaw configuration similar to devices currently in surgical use, and performance tests were conducted on sealing of porcine renal blood vessels, *ex vivo*.

2 Prototype Design and Simulations

2.1 Linear Beam Shaping

A standard laparoscopic probe consisting of a 30-cm length, 5-mm outer-diameter shaft, and 20-mm length jaw was chosen as the design constraint. The multimode optical fiber was designed to deliver the laser energy down the shaft to the jaw where beam shaping optics generated a line beam (18-mm length, 1.2-mm width) along the mouth of the jaw, parallel to the fiber and shaft. A sapphire window with dimensions of 19 mm length $\times$ 2 mm width $\times$ 0.5 mm thick (Meller Optics, Providence, Rhode Island) was added to prevent contamination of the optics from the surrounding fluid environment in the body. The reflective optics selected were designed to transform

a high-power fiber output at a 90 deg angle into a long, linear beam with roughly even power distribution within a constraint of 2×3 mm cross-section, corresponding to the inner volume of the bottom jaw.

The optics was required to handle high laser power (up to 110 W) over a small area, so a metallic mirror was preferred over a beam splitter or diffraction grating. A cylindrical mirror with radius of curvature close to the diameter of the incident collimated beam was used to generate a linear beam directed at an angle of 90 deg. However, use of a single mirror would require too great of a working distance to convert a 1-mm-diameter circular beam to a 20-mm-length linear beam. Therefore, a design consisting of multiple cylindrical mirrors analogous to a "washboard," with short radii arranged along the length of the jaw, tilted upward like a small angle "staircase," was chosen to provide the beam length required (Fig. 1).

2.2 Simulations

A range of cylindrical diameters (0.5, 0.75, and 1 mm), fiber tilts (5 deg, 0 deg, −5 deg), and positions ($H = 0.5$, 0.75, 1, 1.25, 1.5 mm) ($D = 0$, 2.5, 5 mm) were modeled to determine the power distribution along the line beam, where "D" was defined
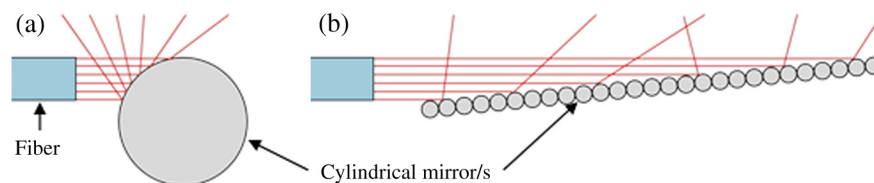

Fig. 1 (a) Side view diagram of fiber illuminating top half of single cylindrical mirror. (b) Washboard-style, multiple cylindrical mirrors arranged in a staircase, creating a longer linear beam directed at 90 deg. Additionally, the shorter height of the optics meets design constraints of the laparoscopic probe jaw.
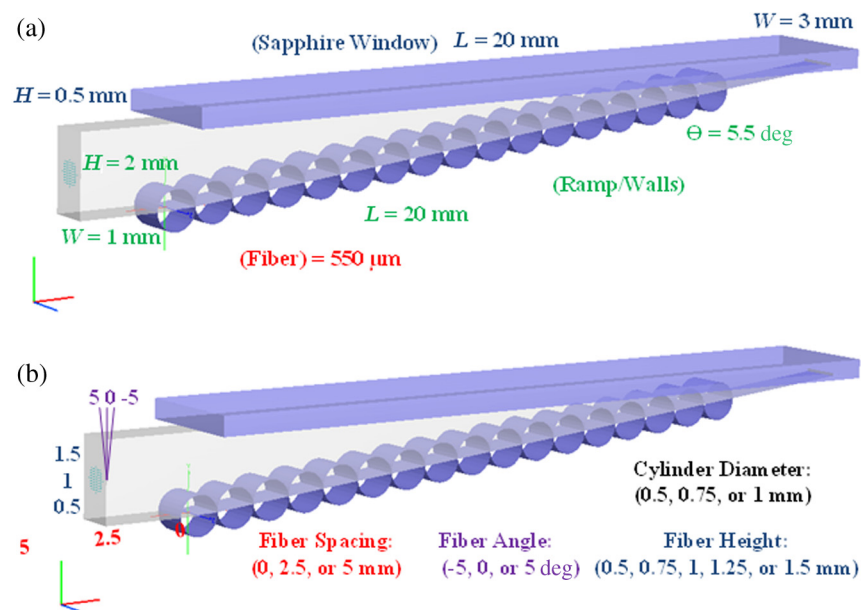

Fig. 2 Three-dimensional layout of FRED simulation showing (a) fixed and (b) variable parameters tested. The uncoated sapphire window ($L = 20$, $W = 3$, $H = 0.5$ mm) rests on top of a reflecting chamber ($W = 1$, $H_{max} = 2$ mm, $\theta_{incline} = 5.5$ deg). The 100% reflecting cylinders are arranged along the incline with the origin at the center of curvature of the first cylinder directly below the proximal edge of the window. The 550-μm-diameter fiber output is directed toward the distal tip and the side walls of the chamber are 100% reflective.
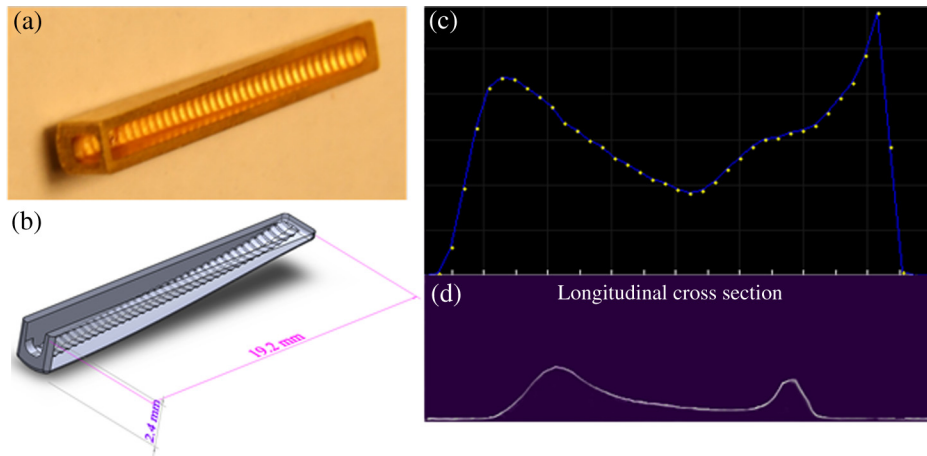
Fig. 3 (a, b) Photograph and diagram of reflective insert with "staircase" geometry placed in lower jaw of laparoscopic prototype; (c) simulation of spatial beam profile; (d) experimental results for spatial beam output of probe.

as the diameter of each reflecting cylinder, and "*H*" as the height of the fiber from the bottom of the reflecting "staircase" design, as labeled in Fig. 2.

Secondary simulations were also carried out using a CAD program (SolidWorks, Dassault Systèmes SolidWorks Corporation, Waltham, Massachusetts). An array of alterations to the geometry was simulated due to manufacturing constraints. Material coatings optical properties (98% reflectivity at 1470 nm for gold and 86% transmission for sapphire glass) were incorporated to provide an accurate simulation result. Photographs and diagrams of the final design and its irradiance profile compared to the experimental tests are provided in Fig. 3. There was a discrepancy between the dimensions of the experimental and simulation results, due to the irradiance being analyzed above the sapphire window for the simulation while the imaging plane of the beam profiler setup was closer to the reflecting insert.

3 Materials and Methods

3.1 Tissue Preparation

Fresh porcine kidney pairs were obtained from a slaughterhouse (Spear Products, Inc., Coopersburg, Pennsylvania) and renal arteries were then dissected, cleaned of fat, and kept hydrated with saline for use within 24 h. The entire vascular tree for each kidney was carefully dissected and surgically exposed in a similar manner to previous studies,[21,22] providing multiple vessels with a wide range of diameters for testing. A total of 69 vessels were tested, ranging from 1.0 to 6.6 mm in diameter and with a mean diameter of 3.3 ± 1.7 mm.

3.2 Laser Parameters

A 100-W, continuous-wave, diode laser with a 1470-nm wavelength (BrightLase Ultra-100, QPC Lasers, Sylmar, California) was chosen, based on previous wavelength optimization studies involving seven different laser wavelengths spanning the infrared spectrum.[21] Since water is a primary absorber of laser radiation in the near- to mid-IR spectrum and soft tissues are composed primarily of water (60% to 80% water content), the optical penetration depth (OPD) can be approximated by the inverse of the water absorption coefficient ($\mu_a = 24$ cm^{-1})

at 1470 nm. The OPD is 0.4 mm, which also closely matches the thickness of the blood vessels, once they are compressed within the jaws of the laparoscopic device, thus providing efficient delivery of optical energy to the vessel.

3.3 Laparoscopic Prototype

A 400-μm-core optical fiber (PN315-0033-001, 0.22 NA, QPC Lasers) connected the laser output to a custom high power fiber optic shutter system (SH-200-55-1470-M-0-T-BH-SP, OZ Optics, Ottawa, Canada). A function generator (DS345, Stanford Research Systems, Sunnyvale, California) precisely controlled the laser pulse duration. Laser energy was delivered through a 550-μm-core-diameter optical fiber (FG550LEC-Custom, Thorlabs, Newton, New Jersey) with high power proximal SMA connector, from the optical shutter output port to the inside of the laparoscopic probe. The laparoscopic prototype with 5-mm-outer-diameter shaft featured a traditional Maryland jaw configuration (Fig. 4). A reflective insert inside of the lower jaw reflected light at an angle of 90 deg to provide a side-delivery interface, with a beam measuring 18-mm-length × 1.2-mm-width. The reflective insert consisted of a series of cylinders placed in a "staircase" like arrangement in which light was incident perpendicular to the cylinders and reflected in a line shape. Figure 3 shows the reflective insert and
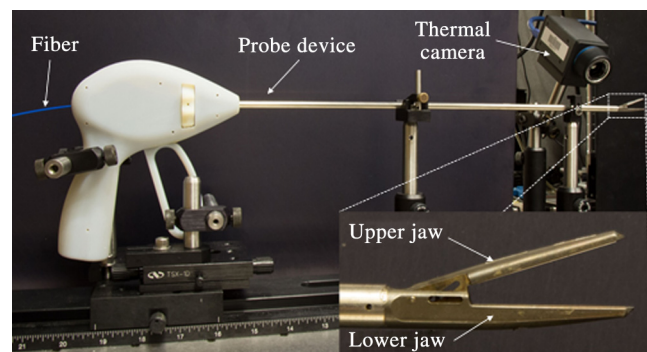

Fig. 4 Prototype device using traditional 5-mm OD Maryland jaw configuration. Insert shows magnified view of upper and lower jaws on the laparoscopic device. Thermal camera was used for noninvasive temperature mapping during the procedure.

a spatial beam profile, acquired using an infrared beam profiler (Pyrocam III, Spiricon, North Logan, Utah). The beam profile provided a pixel count, and knowledge of the size of each pixel and the magnification used enabled calculation of the beam dimensions. A sapphire window (SCD3955, Meller Optics, Providence, Rhode Island) was placed above the insert, and silicone adhesive was used to create an air and watertight seal, ensuring minimal particle and fluid contamination of the insert. An aluminum insert was also used in the upper jaw to provide a backstop for the light and to compress the tissue sample.

3.4 Vessel Sealing Setup

During experiments, porcine vessels were placed in between the bottom and top jaw, and then compressed to the maximum compression allowed by the probe. Once compressed, vessels were irradiated at 68.3 W for 3 s, with light delivered from the lower jaw. The vessel and jaw temperatures were monitored and recorded by a thermal camera (A65, FLIR, Wilsonville, Oregon). The data were then collected and analyzed by the camera software (ResearchIR, FLIR) on a personal computer. Vessel location on jaw, vessel diameter, and degree of desiccation, sticking, and charring were recorded for each vessel. Photographs were also taken before and after laser irradiation of each tissue sample to measure thermal damage.

3.5 Burst Pressure Measurements

Vessel burst pressure measurements were used as the primary indicator for measuring vessel strength and success. The standard burst pressure setup consisted of a pressure meter (Model 717 100 G, Fluke, Everett, Washington), infusion pump (78-01000C, Cole Parmer, Vernon Hills, Illinois), and an iris clamp (Fig. 5). The vessel lumen was placed over a cannula attached to the infusion pump. An iris was then closed to seal the vessel onto the cannula. Deionized water was infused at a rate of 100 ml/h and pressure was measured with the meter. Maximum pressure (mmHg) achieved when the vessel seal burst was then recorded. Although there is no universally accepted standard baseline burst pressure for measuring successful seals in the laboratory, for the purposes of this preliminary feasibility study, a seal was considered successful if it exceeded the physiological values for both normal systolic blood pressure (120 mmHg) and malignant hypertension blood pressure (180 mmHg). A total of 69 vessels were tested and the mean
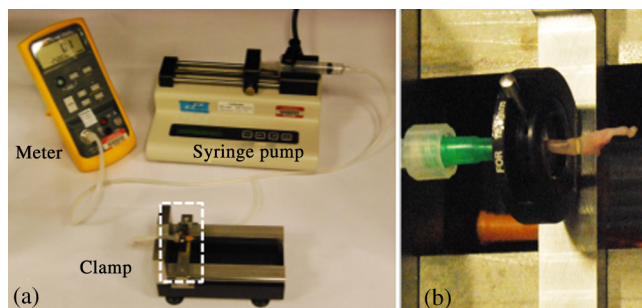

Fig. 5 (a) Burst pressure experimental setup; (b) an iris was used to clamp vessels to a needle, which were then filled with deionized water until the seal burst. Pressure before burst was recorded using a pressure meter.
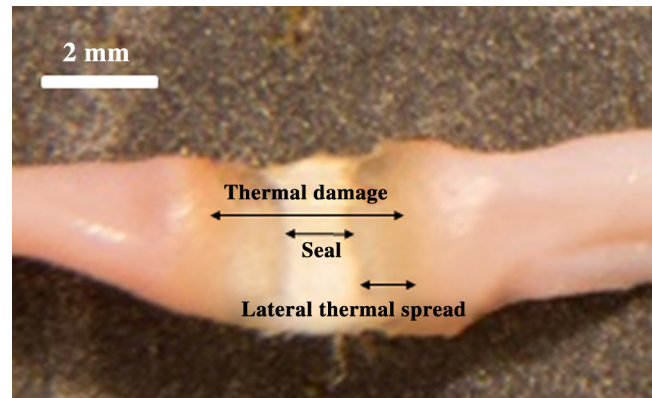

Fig. 6 A vessel sample with seal width (1.1 mm), thermal damage (3.8 mm), and lateral thermal spread (1.4 mm) labeled.

and standard deviation of burst pressures was then calculated for different vessel sizes.

3.6 Thermal Damage Measurements

Measurements of the seal width, thermal damage width, and lateral thermal spread (defined as total thermal damage zone minus seal width, divided by two) were taken from photographs of gross images of each vessel after laser irradiation, with a clear delineation or transition from native to thermally coagulated zones in the samples, as shown in Fig. 6, and consistent with previous studies.[21] Such gross images have been shown to correlate well with histologic analysis provided in previous studies.[22,23]

4 Results

Figure 7 shows a graph of vessel burst pressure (mmHg) data for all 69 vessels tested, as a function of vessel size (mm), with the normal systolic blood pressure (120 mmHg) and malignant hypertension blood pressure (180 mmHg) labeled with dotted and dashed lines, respectively. The mean burst pressure was 1038 ± 474 mmHg for vessels smaller than 5-mm-diameter, with 48/51 successful seals, providing a 94% success rate. Vessels larger than 5 mm were not sealed consistently (6/18), yielding a success rate of only 33%, and a mean burst pressure of only 174 ± 221 mmHg, which was statistically significant compared to the burst pressures for the successful seal ($P < 0.01$).

Representative images of successful seals of small, medium, and large vessels both before and after laser irradiation are shown in Fig. 8. Using gross images from each seal, the total width of the seal, thermal damage zone, and thermal spread were measured to be 1.7 ± 0.8, 3.4 ± 0.7, and 1.0 ± 0.4 mm, respectively. Comparison of these values yielded statistically significant differences ($P < 0.01$).

A thermal image of the probe jaw with a vessel being irradiated is shown in Fig. 9. A peak temperature greater than 135°C (the temperature limit of the camera) was recorded inside the lower jaw. However, a peak temperature of only 57°C was recorded on the outside surface of the upper jaw. Figure 10 shows plots of temperature as a function of time for both the upper and lower jaws for the specific placement of the jaws displayed in Fig. 9. The sharp decrease in temperature shown in Fig. 9(b) at time, $t = 25$ s, is an artifact due to movement of the jaw to remove the vessel after laser irradiation, in accordance with the standard protocol for vessel sealing.
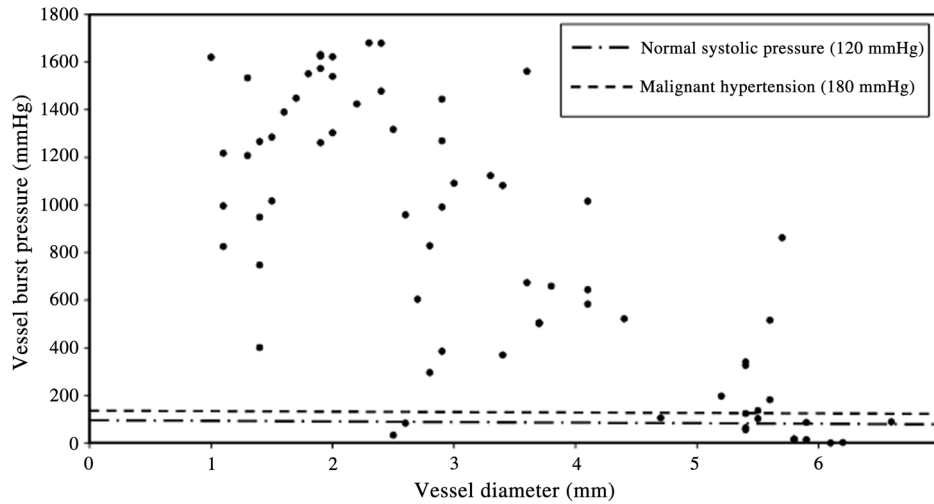
Fig. 7 Burst pressure as a function of vessel diameter ($n = 69$), with normal systolic blood pressure (120 mmHg) and malignant hypertension blood pressure (180 mmHg) labeled.
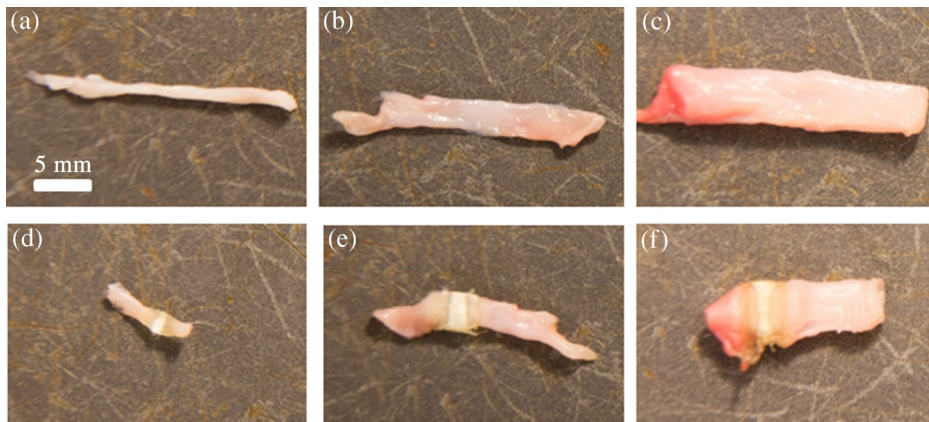

Fig. 8 The top and bottom rows show representative images of vessels before and after successful seals were achieved for small, medium, and large vessel diameters (d): (a, d) $d = 1.2$ mm; (b, e) $d = 3.1$ mm; and (c, f) $d = 5.3$ mm.
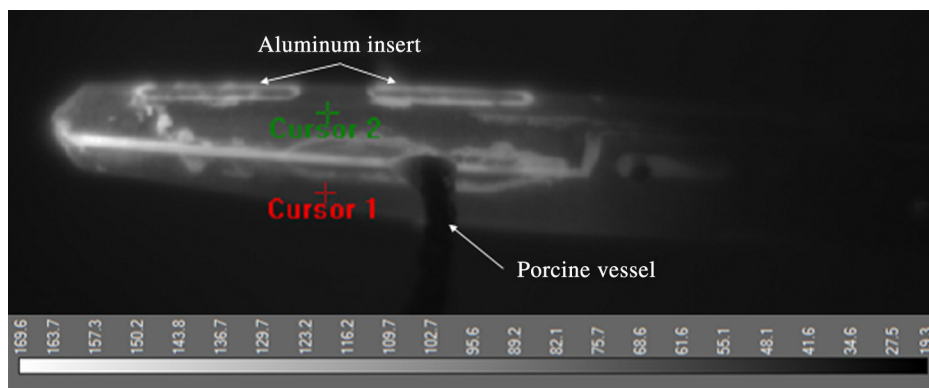

Fig. 9 Thermal image of jaw acquired at time of peak detected temperature inside of the jaw (>135°C). The figure uses a false color image scale, with lightest color corresponding to highest temperature (>135°C) and darkest corresponding to lowest temperature (20°C).

5 Discussion

The main objective of this study was to determine the feasibility of infrared laser vessel sealing using an optical laparoscopic prototype with a 5-mm outer-diameter shaft integrated within a Maryland jaw design currently used in the clinic with RF energy-based instruments. The optical prototype was successful in sealing vessels less than 5 mm with a 3-s irradiation time, on par with current clinical RF and US energy-based devices that
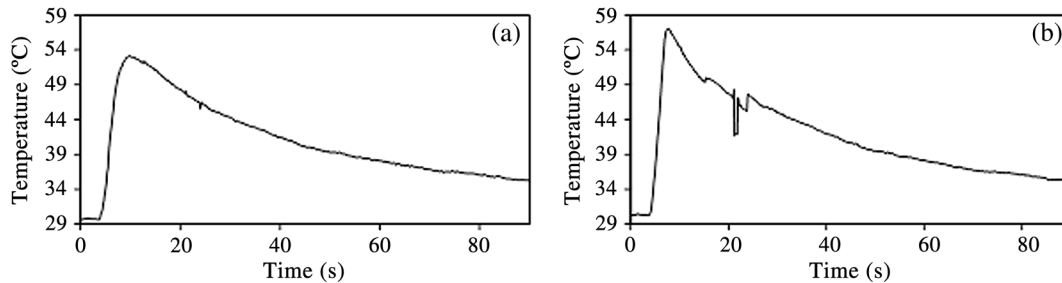
Fig. 10 Temperature versus time graphs for outside surface of (a) lower and (b) upper jaws. The exact locations can be seen labeled as cursor 1 and 2 in Fig. 9. The abrupt drop in temperature shown in (b) at $t = 25$ s is due to movement of the jaw to remove the vessel after laser irradiation.

typically take 3 s or greater to seal and cut vessels.[24] While most vessels less than 5 mm were successfully sealed, two vessels failed both criteria and one vessel failed the burst pressure threshold for malignant hypertension (Fig. 7). Vessels that failed both criteria had diameters of about 2.5 mm and were inadvertently sealed at a bifurcation or branch between them and another vessel. Based on our previous experiences, when such a branch is sealed instead of a single vessel, multiple weak points are created where the seal can potentially burst at a much lower pressure than vessels sealed at locations other than branches.

There was limited success for vessels greater than 5-mm diameter, possibly due to several factors. First, all vessels over 5 mm were dissected from the main renal artery. These vessels were more rigid and had significantly greater wall thicknesses and possibly higher collagen content as well. Second, the thicker vessel walls made it more difficult for the probe to create equal pressure across the vessel, which left a large gap at the distal tip of the jaw. There may have also been variability in the pressure that each vessel experienced, since the pressure could not be actively measured. In future studies, higher incident laser power may be used to facilitate better sealing of vessels measuring greater than 5 mm.

Temperatures recorded on the outside surfaces of both the lower and upper jaws of the optical prototype peaked at less than 60°C. This value is well below the peak temperatures of current clinical energy-based devices. For example, temperatures greater than 200°C for US devices and near 100°C for RF devices have been reported.[9,10] Although jaw cooling times were relatively slow for the optical prototype, as shown in Fig. 10, the low peak temperatures recorded should translate into minimal waiting times in between device applications during a surgical procedure, and hence potentially a more expedited procedure as well. Furthermore, if future studies with our laparoscopic prototype are able to replicate the 1-s sealing times reported during our previous work using a benchtop setup,[22] this may also translate into even lower peak temperatures and correspondingly lower cooling times between applications as well. However, this remains to be explored further in future studies.

Seal widths, thermal damage zones, and thermal spread measured 1.7 ± 0.8, 3.4 ± 0.7, and 1.0 ± 0.4 mm, respectively, with the optical prototype. Lateral thermal spread is of concern during surgery, due to the potential for unintended thermal damage to adjacent critical tissue structures when performing delicate procedures in confined spaces (e.g., prostatectomies and thyroidectomies). For the optical prototype, the values for thermal spread were similar to those previously reported for US and RF energy-based devices.[22]

It should also be noted that laboratory testing of energy-based devices for vessel sealing is limited to arteries, not veins, for several reasons. First, arteries are required to withstand significantly higher physiological pressures than veins. Second, arteries are composed of thick, muscular walls, providing a worst case scenario in terms of resistance to compression and higher energy requirements for sealing. Third, veins are delicate and fragile once blood flow has ceased, making them difficult to dissect *ex vivo*. Therefore, veins are only evaluated *in vivo* under appropriate physiological conditions. There is some literature suggesting that burst pressures for arteries are higher than for veins, while thermal spread is greater in veins than arteries, after sealing with energy-based devices in a pig model *in vivo*.[25] Perhaps the thicker artery walls provide more tissue for coagulation resulting in higher burst pressures than for veins. Greater thermal spread along the length of the veins may be necessary to create a successful seal.

Our previous laboratory studies demonstrated sealing and cutting times as short as 1 s.[22] The current prototype did not facilitate cutting, but future work will be directed at enabling this additional capability, as well as continuing to explore the potential of achieving shorter seal times in the laparoscopic device. Future laparoscopic probe designs may also implement a two-step sealing and cutting technique to bisect vessels after they are sealed, similar to what was reported with earlier versions of a laser-based vessel sealing prototype.[22] This may be achieved through several different approaches. Modified geometries of the reflector as well as the sapphire window will be investigated to increase power density and applied force to facilitate bisection of the sealed vessel. Increasing laser power for cutting following the seal creation will also be investigated. Additional studies in a porcine model will be conducted to determine *in vivo* performance of the laparoscopic probe. The ability to maintain hemostasis after sealing and transecting abdominal and hind leg vasculature will be evaluated, and lateral thermal spread will be measured using histology.

6 Conclusions

An optical laparoscopic prototype with 5-mm outer-diameter shaft integrated within a standard Maryland jaw configuration consistently sealed vessels less than 5-mm diameter with low lateral thermal spread. Further *in vivo* pig studies are planned on a variety of vessels and vessel bundles.

Disclosures

References

1. Z. Ding, M. Wable, and A. Rane, "Use of Ligasure bipolar diathermy system in vaginal hysterectomy," *J. Obstet. Gynaecol.* **25**(1), 49–51 (2005).
2. B. Levy and L. Emery, "Randomized trial of suture versus electrosurgical bipolar vessel sealing in vaginal hysterectomy," *Obstet. Gynecol.* **102**(1), 147–51 (2003).
3. C. Leonardo et al., "Laparoscopic nephrectomy using Ligasure system: preliminary experience," *J. Endourol.* **19**(8), 976–978 (2005).
4. P. Manasia, A. Alcaraz, and J. Alcover, "Ligasure versus sutures in bladder replacement with Montie ileal neobladder after radical cystectomy," *Arch. Ital. Urol. Androl.* **75**(4), 199–201 (2003).
5. F. Romano et al., "Laparoscopic splenectomy: ligasure versus EndoGIA: a comparative study," *J. Laparoendosc. Adv. Surg. Tech. A.* **17**(6), 763–768 (2007).
6. P. W. Marcello et al., "Vascular pedicle ligation techniques during laparoscopic colectomy. A prospective randomized trial," *Surg. Endosc.* **20**(2), 263–269 (2006).
7. http://www.ethicon.com/healthcare-professionals/products/energy-devices/harmonic-ace-plus
8. http://surgical.covidien.com/products/ultrasonic-dissection/sonicision.
9. C. K. Phillips et al., "Tissue response to surgical energy devices," *Urology* **71**(4), 744–748 (2008).
10. F. J. Kim et al., "Temperature safety profile of laparoscopic devices: harmonic ACE (ACE), Ligasure V (LV), and plasma trisector (PT)," *Surg. Endosc.* **22**(6), 1464–1469 (2008).
11. M. Garancini et al., "Bipolar vessel sealing system vs. clamp crushing technique for liver parenchyma transaction," *Hepatogastroenterology* **58**(105), 127–132 (2011).
12. A. Stoff, M. A. Reichenberger, and D. F. Richter, "Comparing the ultrasonically activated scalpel (Harmonic) with high-frequency electrocautery for postoperative serious drainage in massive weight loss surgery," *Plast. Reconstr. Surg.* **120**(4), 1092–1093 (2007).
13. Y. Kurt et al., "New energy-based devices in laparoscopic splenectomy: comparison of Ligasure alone versus Ligasure and Ultracision together," *Surgical Pract.* **16**(1), 28–32 (2012).
14. Y. Pons et al., "Comparison of LigaSure vessel sealing system, harmonic scalpel, and conventional hemostasis in total thyroidectomy," *Otolaryngol. Head Neck Surg.* **141**(4), 496–501 (2009).
15. J. Kroft and A. Selk, "Energy-based vessel sealing in vaginal hysterectomy: a systematic review and meta-analysis," *Obstet. Gynecol.* **118**(5), 1127–1136 (2011).
16. M. Adamina et al., "Randomized clinical trial comparing the cost and effectiveness of bipolar vessel sealers versus clips and vascular staplers for laparoscopic colorectal resection," *Br. J. Surg.* **98**(12), 1703–1712 (2011).
17. J. Landman et al., "Evaluation of a vessel sealing system, bipolar electrosurgery, harmonic scalpel, titanium clips, endoscopic gastrointestinal anastomosis vascular staples and sutures for arterial and venous ligation in a porcine model," *J. Urol.* **169**(2), 697–700 (2003).
18. G. W. Hruby et al., "Evaluation of surgical energy devices for vessel sealing and peripheral energy spread in a porcine model," *J. Urol.* **178**(6), 2689–2693 (2007).
19. G. R. Lamberton et al., "Prospective comparison of four laparoscopic vessel ligation devices," *J. Endourol.* **22**(10), 2307–2312 (2008).
20. P. A. Sutton et al., "Comparison of lateral thermal spread using monopolar and bipolar diathermy, the Harmonic scalpel, and the Ligasure," *Br. J. Surg.* **97**(3), 428–433 (2010).
21. C. M. Cilip et al., "Infrared laser thermal fusion of blood vessels: preliminary ex vivo tissue studies," *J. Biomed. Opt.* **18**(5), 058001 (2013).
22. N. C. Giglio et al., "Rapid sealing and cutting of porcine blood vessels, *ex vivo*, using a high power, 1470-nm diode laser," *J. Biomed. Opt.* **19**(3), 038002 (2014).
23. C. M. Cilip et al., "Infrared laser sealing of porcine vascular tissues using a 1470 nm diode laser: preliminary in vivo studies," *Lasers Surg. Med.* **49**(4), 366–371 (2017).
24. W. L. Newcomb et al., "Comparison of blood vessel sealing among new electrosurgical and ultrasonic devices," *Surg. Endosc.* **23**(1), 90–96 (2009).
25. S. Richter et al., "Differential response of arteries and veins to bipolar vessel sealing: evaluation of a novel reusable device," *J. Laparoendosc. Adv. Surg. Tech. A.* **16**(2), 149–155 (2006).

Luke A. Hardy is currently a PhD student in the Optical Science and Engineering Program at the University of North Carolina at Charlotte, NC.

Thomas C. Hutchens, PhD, is currently a postdoctoral fellow in the Department of Physics and Optical Science at the University of North Carolina at Charlotte, NC.

Eric R. Larson is a senior engineering manager for R&D at Medtronic in Boulder, CO.

David A. Gonzalez is currently an undergraduate physics major at the University of North Carolina at Charlotte, NC.

Chun-Hung Chang is currently a PhD student in the Optical Science and Engineering Program at the University of North Carolina at Charlotte, NC.

William H. Nau, PhD, is a distinguished scientist with the Medtronic Surgical Innovations Group in Boulder, CO.

Nathaniel M. Fried, PhD, is currently a professor in the Department of Physics and Optical Science at the University of North Carolina at Charlotte and an adjunct faculty member in the McKay Department of Urology at Carolinas Medical Center in Charlotte, NC. His research interests include therapeutic and diagnostic applications of lasers in urology.